High activity and stability of the Rh-free Co-based ex-hydrotalcite containing Pd in the catalytic decomposition of N_2O

Javier Pérez-Ramírez *, Freek Kapteijn and Jacob A. Moulijn

Industrial Catalysis, DelftChemTech, Delft University of Technology, Julianalaan 136, 2628 BL Delft, The Netherlands
E-mail: j.perez@stm.tudelft.nl

Received 29 March 1999; accepted 20 May 1999

The catalytic decomposition of nitrous oxide to nitrogen and oxygen has been studied over calcined hydrotalcite-like compounds containing different combinations of bivalent (Co, Pd, Mg) and trivalent (Al, La, Rh) cations with carbonate as interlayer anion. The precursors were prepared by co-precipitation under low supersaturation conditions and characterized by XRD and TG/DSC. The mixed oxides derived after calcination at 723 K were characterized by XRD, N_2 adsorption at 77 K, and XRF. The presence of Rh, La, or Pd in the Co-based HTlc's improves considerably the catalytic activity. Co–Rh,Al-HTlc (Co/Rh/Al $=$ 3/0.02/1) proved to be a very active catalyst, although the presence of the noble metal Pd in this catalyst ex-Co,Pd–La,Al-HT (Co/Pd/La/Al $=$ 3/1/1/1) produces a similar catalytic activity to that of Rh-containing catalyst, both in a N_2O-containing stream and in one containing also SO_2 and O_2, but with a better performance in stability tests. PdO phase has been identified by XRD as being responsible for the considerable improvement in the activity. The presence of Mg as spinel structure exerts a stabilizing effect in the more active catalysts when mixtures of SO_2 and O_2 are considered.

Keywords: N_2O decomposition, calcined HTlc's, cobalt spinel, palladium, rhodium, lanthanum, magnesium aluminate, Mg stabilization, SO_2 poisoning

1. Introduction

The well-known environmental problem caused by nitrous oxide, N_2O, as greenhouse effect gas and ozone layer depletor [1–3], requires the urgent reduction of its emissions, especially those from the point sources like stationary combustion and chemical production processes. Catalytic decomposition of N_2O offers an attractive alternative as *end-of-pipe* solution in these situations [4]. The low operation temperature of the catalysts is of special importance for practical applications, due to the high potential energy costs involved in heat transfer operations. Generally, the most active catalytic systems at low temperatures are those containing Rh, either in zeolites [5–7], supported oxides [6–9], or calcined hydrotalcites [10–13]. In the last group, different authors have reported that the presence of Rh in Co- or Zn-based catalysts improves dramatically the catalytic activity even in industrial-like conditions [14]. However, the high cost of the noble metal Rh can become limiting for industrial applications. Pd-ZSM-5 has been reported as a very active catalyst for the decomposition of N_2O, even more than the well-known Cu-ZSM-5 [5], but not much attention has been paid when applied in supported oxides or mixed oxides. Hydrotalcite-like compounds (HTlc's) are potential multicomponent precursors where several di- or trivalent cations can be placed. In our previous work [13], we had considered La as an alternative, achieving a considerable increase in the catalytic activity with respect to the Co-based mixed oxide, but not as much as with Rh.

This paper considers the addition of different cations (bivalents and/or trivalents) in order to obtain a less expensive catalytic system based on Co-hydrotalcites approaching the activity of that containing Rh.

2. Experimental

2.1. Catalyst preparation

Hydrotalcite-like materials $[M^{2+}_x M^{3+}_{1-x}(OH)_2]^{x+}\cdot[CO_3^{2-}]_{x/2}\cdot mH_2O$ used here were prepared by a standard aqueous co-precipitation method at constant pH, temperature and heat of crystallization [15]. A flow (2 l/h) of an aqueous solution of the metal nitrates in a desired molar ratio with a total cation ($M^{2+} + M^{3+}$) concentration of 1.5 M was mixed slowly at room temperature under vigorous agitation with an alkaline solution of Na_2CO_3/NaOH, with the carbonate concentration in the molar ratio $CO_3^{2-}/Al^{3+} = 2$. The pH of the mixtures was kept at 10, by adjusting the flow rate of the alkaline solution. Following this addition the slurry was aged at 338 K for 18 h under mild stirring. Finally, the material was cooled to room temperature, filtered, washed with warm (303 K) deionized water, and dried at 363 K for 12 h. The hydrotalcites were calcined for 18 h in static air raising the temperature to 723 K at a rate of 10 K/min. These samples are indicated as ex-HTlc's.

---

[*] To whom correspondence should be addressed.

2.2. Catalyst characterization

The decomposition of the HTlc's for the determination of the optimal calcination temperature was studied by TG/DSC in a Thermal Science STA 1500H apparatus. The temperature range was 300–900 K, using a heating rate of 10 K/min in air. Nitrogen adsorption was carried out to determine the specific surface and total pore volume of the calcined samples. For this purpose, the samples were pre-treated under vacuum at 623 K for 16 h. The surface area was measured employing the BET adsorption method in Autosorb-6B from QuantaChrome sorptometer at 77 K. The XRD were taken in a Philips PW 1840 X-ray diffractometer, using Cu K_α radiation with silicon as internal standard with $\lambda = 0.1541$ nm at a scan speed of $3^\circ\,\mathrm{min}^{-1}$. The data obtained were scaled and the crystallite size was calculated from the line broadening of the maximum reflection for each pattern using the Scherrer formula [16]. The chemical composition of the calcined materials was determined by XRF in a Philips PW 1480 apparatus, in order to compare the molar ratio of cations used in the preparation to that observed in the sample.

2.3. Experimental set-up and procedures

The reaction of N_2O decomposition was performed in a quartz-tube fixed-bed reactor of 5 mm i.d. under the conditions of 1 mbar N_2O in He in the 450–750 K temperature range. 50 mg of catalyst diluted with 150 mg of SiC was used for each run and the flow rate of the feed gas was 100 ml/min STP (space time $W/F^0_{N_2O} = 8.05 \times 10^5$ g s/mol). The SiC diluent did not contribute to the N_2O decomposition at the reaction temperatures studied. Stability tests were performed at constant temperature by passing a flow containing 1 mbar N_2O in He. The sensitivity for mixtures containing SO_2 and O_2 was checked by adding 0.125 mbar SO_2 and 30 mbar O_2 in the stream containing 1 mbar N_2O in He during 1 h. Prior to each run, each catalyst was pretreated in He at 723 K for 1 h. Generally, 60 min after a change of conditions the N_2O conversion levels were constant and considered as the steady state. Mass and heat transport limitations in the reactor were absent [17]. The product gases were discontinuously analyzed for N_2O, N_2, and O_2 by GC equipped with TCD and ECD detectors, using a Poraplot Q column and a Molsieve 5A column for separation [18].

3. Results and discussion

3.1. Catalyst characterization

Table 1 lists the samples prepared and the results of the characterization. XRF revealed that the ratio between cations in the calcined samples was close to that in the starting solutions, proving that the coprecipitation step was carried out effectively. All precursors crystallized in the single phase with hydrotalcite structure HT (hexagonal system), exhibiting sharp and symmetric peaks for the (003), (006), (009), (110), and (113) planes and broad and asymmetric peaks for the (102), (105), and (108) planes characteristic of clay minerals having a layered structure [19]. The patterns of similar HTlc's reported in the literature [20,21] corresponded with those from these precursors. Obviously, the lattice parameters a and c of the different precursors differ slightly due to the different sizes (ionic radii) of the cations considered.

TG/DSC decomposition profiles of the precursors show the presence of two endothermic peaks and two stages of weight loss, providing an additional proof of the achievement of the HT structure [21,22]. Globally, the total weight loss for the samples was between 25 and 35%. The first weight loss stage occurs between 400 and 500 K and the second weight loss stage between 500 and 650 K (except for the La-based catalysts). The temperatures and peak intensities changed for each sample, due to different electrostatic interactions between layers and interlayers [23] and the different bond strength in the basic layers associated with the different compounds and compositions. For ex-Co–Rh,Al-HTlc, the endothermic peaks for both transitions mentioned nearly merged, being an indication of their simultaneous occurrence. For the La-containing catalysts,

Table 1
Data on catalysts used in the present study.

Catalyst	Atomic molar ratio		Precursor[a]	After calcination at 723 K			
	Solution	Solid		S_{BET} (m^2/g)	V_p (cm^3/g)	$d_{crystal}$ (nm)	Phases identified
Co–Al-HTlc	3/1	2.9/1	HT	140	0.60	90	Spinel
Co–Rh,Al-HTlc	3/0.02/1	3.1/0.02/1 (0.7 wt% Rh)	HT	120	0.75	100	Spinel
Co,Mg–Rh,Al-HTlc	3/1/0.02/1	3.1/1/0.02/1 (0.7 wt% Rh)	HT	150	0.75	80	Spinel
Co–La,Al-HTlc	3/1/1	2.9/1/1	HT	100	0.40	85	Spinel, La_2O_3, La_2CO_5
Co,Pd–La,Al-HTlc	3/0.01/1/1	2.9/0.01/0.9/1 (0.3 wt% Pd)	HT	105	0.40	80	Spinel, La_2O_3, La_2CO_5
Co,Pd–La,Al-HTlc	3/1/1/1	2.8/0.9/1/1	HT	95	0.50	75	Spinel, La_2O_3, La_2CO_5, PdO
Co,Mg,Pd–La,Al-HTlc	3/1/1/1/1	2.9/1/0.9/0.8/1	HT	100	0.55	70	Spinel, La_2O_3, La_2CO_5, PdO

[a] HT: hydrotalcite.

the second weight loss has shifted about 100–150 K to higher temperatures, suggesting that this system is more stable upon heating than the other HTlc's. The addition of Pd (in both molar ratios Pd/Al 0.01 and 1) to this catalyst produces similar profiles, while the presence of Mg provokes a second weight loss stage slightly larger, with the first stage being practically the same. Based on this thermal analysis, the calcination temperature for the activation of the HTlc's before the activity tests was chosen to be 723 K. At this temperature, carbonate elimination seems to be complete and the presence of more endothermic peaks, belonging to the reaction among mixed oxides causing their sintering with phase segregation was not identified. The calcination step results in the destruction of the layered structure and in the formation of high surface area, non-stoichiometric, highly disordered and well-dispersed mixed metal oxides [24]. The homogeneous interdispersion of the elements in the calcined samples, producing an isotropic material with atomic scale dispersion, has been detected by ^{27}Al MAS-NMR with ex-Co–Rh,Al-HTlc, where a very sharp peak at 13 ppm and no spinning side band signal have been observed [25]. This band is assigned to Al octahedrally coordinated with oxygen in the mixed oxide. The presence of Al tetrahedrally coordinated has also appeared at 70 ppm, being in agreement with the results reported in literature for ex-Mg–Al-HTlc [26].

The phases identified by XRD after calcination of the HTlc's are indicated in table 1 and figure 1. In all the samples, Co-based spinel-like structures may be observed, like $CoAl_2O_4$, Co_2AlO_4 or Co_3O_4, but due to the similar reflection angles and intensities, it is not possible to distinguish between them. It is more likely to have $CoAl_2O_4$ than Co_2AlO_4, due to the tendency of cobalt to form normal spinel structures, although some degree of inversion has been detected, especially when Mg is present in the catalyst [27]. However, the main factor leading to the inversion is the quenching temperature. The relatively low calcination temperatures will favour the location of cobalt in tetrahedral positions in the cubic close packed structure [28]. The single oxide CoO or Co_2O_3 is not identified by XRD in the catalyst, confirming that the active cobalt is located in a spinel-like structure. From the broadening of the major XRD reflection an estimate of the crystal size is made, which is included in table 1. In lanthanum-based catalysts (figure 1(d) and (e)), peaks corresponding with lanthanum oxide carbonate phases can be observed at low reflection angles, mainly La_2CO_5, which possesses tetragonal structure. Additionally, the single oxide La_2O_3 has been identified. The catalyst containing Pd in small amounts (Co/Pd/La/Al = 3/0.01/1/1) shows a similar behaviour as the ex-Co–La,Al-HTlc (figure 1(d)), with no Pd-related phase. However, the addition of larger amounts of Pd (Co/Pd/La/Al = 3/1/1/1), produces a crystallographic Pd phase which can be easily identified at $2\theta = 34^\circ$. This reflection has been assigned to PdO, being the most intense reflection. The main reflection observed is broad, accounting for a small crystallite size (see figure 1(e)). The rest of reflections for this crystallographic phase are weak. The presence of other possible Pd-related phases has been checked for the assignment of the sharp effect observed in the catalytic activity for the N_2O decomposition. The spinel-like structure $PdAl_2O_4$ or the mixed oxide with both metals in the same oxidation state $PdCoO_2$ were not identified in the pattern. La_4PdO_7 can also be excluded, and $LaPdO_4$, although unlikely, could be present in small amounts because it possesses sharp reflections at $2\theta \approx 30^\circ$, but at this angle the appearance of the sharper reflection of the lanthanum oxide carbonate is produced. On the other hand, the relatively low calcination temperature (723 K) impedes the formation of metallic palladium by PdO decomposition at high temperatures, namely 1173 K [29].

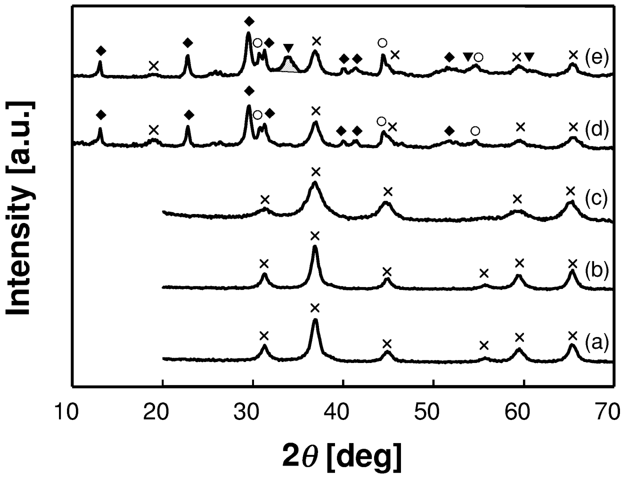

Figure 1. XRD patterns of some calcined hydrotalcite samples: (a) ex-Co–Al-HTlc (Co/Al = 3/1), (b) ex-Co–Rh,Al-HTlc (Co/Rh/Al = 3/0.02/1), (c) ex-Co,Mg–Rh,Al-HTlc (Co/Mg/Rh/Al = 3/1/0.02/1), (d) ex-Co–La, Al-HTlc (Co/La/Al = 3/1/1), and (e) ex-Co,Pd–La,Al-HTlc (Co/Pd/La/Al = 3/1/1/1). Phases identified: (×) Co spinel, (♦) La_2CO_5, (○) La_2O_3, and (▼) PdO.

In general, the calcined hydrotalcites show large specific surface areas. These have resulted to be twice as high in comparison with the results reported previously by Kannan et al. [10], although the trend is similar. The difference might well be due to the different conditions during the preparation of the hydrotalcite. As can be seen in table 1, the presence of Mg improves this surface area, acting as structural promoter for the Co-based catalysts [13]. From the XRD patterns it can be deduced that the presence of Mg in the Co-based calcined catalyst gives rise to a broadening of the diffraction peaks indicating smaller crystallite sizes (figure 1(c)). This will yield generally larger specific surface areas. Mg is forming a spinel-like structure (magnesium aluminate), although the reflections are not identified separately due to the coincidence with the d values of the Co-based spinels [13].

The presence of the oxocarbonate phases in the structure of the calcined product containing La, the relatively high temperature at which the second transition takes place in the TG/DSC experiments, and the lower surface areas, evidence the deviating behaviour of the La-based catalysts. The large ionic radius of the La^{3+} (106 pm) with respect to that of Al^{3+} (45 pm) is affecting the catalyst structure, producing a material which digresses from the common behaviour. Lanthanum could be partially located in the surface of the catalyst, explaining the slightly lower surface area. On the other hand, the patterns of ex-Co–Al-HTlc and ex-Co–Rh,Al-HTlc were identical, probably due, partly, to the small amounts of Rh in the calcined HTlc and to the fact that the ionic radius of Rh^{3+} (68 pm) differs not much from that of Al^{3+}. Consequently, Rh can substitute for Al in the HTlc structure without distorting significantly its constitution, like has been shown for Ru [30].

3.2. Catalytic activity

3.2.1. N_2O in He

Figure 2 shows the influence of the temperature on the conversion of nitrous oxide for different samples. All catalysts were tested at increasing and decreasing temperature ramps in order to check for deactivation or activation. No significant differences in this respect were detected. A dramatic improvement is observed in the conversion after the addition of different cations (bivalent and/or trivalent) to the ex-Co–Al-HTlc. The shapes of all these curves indicate a different temperature dependency for the catalysts, demonstrating different apparent activation energies. Ex-Co–Rh,Al-HTlc (Co/Rh/Al = 3/0.02/1) is more active than ex-Co–La,Al-HTlc (Co/La/Al = 3/1/1). The addition of Pd to the La-containing ex-HTlc produces different results, depending on the Pd loading. A slight effect in the activity has been detected when Pd is added in a molar ratio Pd/Al = 0.01, which is comparable to the Rh loading in the ex-Co–Rh,Al-HTlc. However, the presence of Pd in a molar ratio Pd/Al = 1 leads to a remarkable improvement, giving a similar result to the Rh-containing catalyst. The addition of the less expensive Pd offers an interesting alternative for the Rh catalyst. Although the amount of Pd in the catalyst is 50 times larger than that of Rh, it is still advantageous to dispose of a catalyst with a relatively higher loading, because the catalytic activity will be less sensitive to poisons, having a wider range of operation in their presence. Additionally, the optimization of the Pd loading has not been carried out, while for the Rh catalysts this has been done [11,12]. Therefore, the optimal Pd loading might lie at lower values.

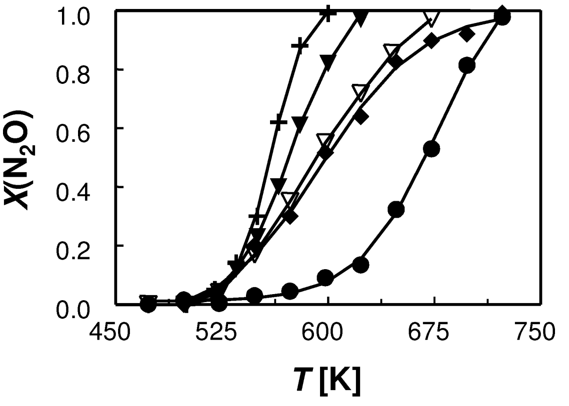

Figure 2. Conversion as a function of temperature at 1 mbar N_2O and space time $W/F^0_{N_2O} = 8.05 \times 10^5$ g s/mol for: (●) ex-Co–Al-HTlc (Co/Al = 3/1), (♦) ex-Co–La,Al-HTlc (Co/La/Al = 3/1/1), (▽) ex-Co,Pd–La,Al-HTlc (Co/Pd/La/Al = 3/0.01/1/1), (▼) ex-Co,Pd–La,Al-HTlc (Co/Pd/La/Al = 3/1/1/1), and (+) ex-Co–Rh,Al-HTlc (Co/Rh/Al = 3/0.02/1).

Careful analysis of the XRD patterns enables the identification of the possible active phases containing the additional cations. In the case of the ex-Co–Rh,Al-HTlc (Rh/Al = 0.02) and ex-Co,Pd–La,Al-HTlc (Pd/Al = 0.01), the low loading of the noble metals makes impossible the identification of Rh- or Pd-related phases. In the case of La-based catalysts, a La_2O_3 phase was found apart from the cobalt spinel-like structures. Therefore, the additional presence of this single oxide, which presents high activities for the N_2O decomposition at even 623 K [31] gives a reasonable explanation for the observed behaviour. Pd-related phase PdO was identified in the ex-Co,Pd–La,Al-HTlc (Co/Pd/La/Al = 3/1/1/1). Pd-based materials have a wide utilisation as total oxidation (CTO) or partial oxidation (CPO) heterogeneous catalysts [32], especially in the total oxidation reaction of methane [33,34]. This application is based on the high oxygen sticking probability, which corresponds to a low value of the activation energy of oxygen chemisorption [35]. Basile et al. [29] have demonstrated that the activity of Pd-based ex-hydrotalcite did not change with time-on-stream even at high temperature, evidencing the stability of this catalyst in an oxidizing atmosphere. The ability of this catalyst for hydrocarbon activation led to a total oxygen conversion. This type of reaction is related to the decomposition of N_2O, where the desorption of the adsorbed oxygen is the most difficult step in the reaction [4]. Therefore, our preliminary interpretation is that the presence of PdO produces a fast rate for O_2 evolution from the solid surface, favouring the process substantially.

3.2.2. Stability

The stability tests performed are shown in figure 3. A slight deactivation is observed for ex-Co–La,Al-HTlc and ex-Co,Pd–La,Al-HTlc. In both cases, the conversion dropped approximately 5% during the first 8 h at the temperatures shown in figure 3. Then it remained constant. After more than 60 h, the temperature was raised to 723 K for 45 min in the presence of an N_2O-free stream. Conversion levels after this treatment were similar to that of the fresh catalysts, indicating that reactivation is possible. On the other hand, for ex-Co–Rh,Al-HTlc, a significant deactivation was measured, exhibited by a conversion drop from 80 to 60% during the first 10 h and stabilizes at approximately 53% until the end of the experiment. For this catalyst, as stated before [13], the presence of Mg in the catalyst avoids the initial deactivation, maintaining the conversion at the initial level during the time-on-stream. The superior behaviour of the ex-Co,Pd–La,Al-HTlc catalyst is clear. The stable behaviour should be attributed mainly to the La-related phases discussed above, which inhibit the deactivation of the Co-based active phase. Further research should be carried out in this respect in order to consolidate this hypothesis, in particular the Pd-based phase may also have importance.

3.2.3. Effect of SO_2 and O_2 mixtures

For the most active catalysts, i.e., those containing Rh, La and Pd, preliminary tests were carried out with a stream containing both 0.125 mbar SO_2 and 30 mbar O_2 in 1 mbar N_2O, in order to check their performance in simulated FBC-like flue-gas conditions. The inhibition by SO_2 and O_2 mixtures is produced by the chemical adsorption of sulfur oxides and formation of sulfates. The presence of Mg in the ex-Co,Mg–Rh,Al-HTlc catalyst improves the resistance against SO_2 at low temperature (595 K) [13]. In view of the potential application of the catalyst ex-Co,Pd–La,Al-HTlc as alternative for the ex-Co–Rh,Al-HTlc, Mg has been incorporated in the catalyst structure. The results are shown in figure 4. At high temperatures (723 and 673 K), both ex-Co–Rh,Al-HTlc and ex-Co,Pd–La,Al-HTlc hardly show any inhibition to SO_2 and O_2. However, at low temperature (595 K), both catalysts are deactivated after exposure to this mixture. Ex-Co,Pd–La,Al-HTlc recovers some activity after removal of the poison from the feed stream, while for ex-Co–Rh,Al-HTlc at 595 K deactivation is close to irreversible. The presence of Mg in these catalysts at low temperatures produces less inhibition during the exposure to SO_2 and O_2, probably due to preferential adsorption on the basic spinel-like structure containing Mg, preserving the active component free for the reaction of N_2O. In this sense, the magnesium aluminate spinel acts as a SO_2 scavenger, as it has been conceived for the SO_x removal in FCC flue gas [36,37]. However, the point to be stressed has no direct relation with this fact, which consists on a stoichiometric reaction, but with the recovery of the activity after removal of the poisons. This result clearly evidences that Mg is playing a stabilizing role in the catalysts, avoiding the irreversible poisoning at low temperature. Although in most cases the amount of SO_2 passed over the catalyst is about ten times smaller than there is active element present (except for Rh), the results demonstrate whether there is a strong inhibition effect or not, and if this is irreversible (poi-

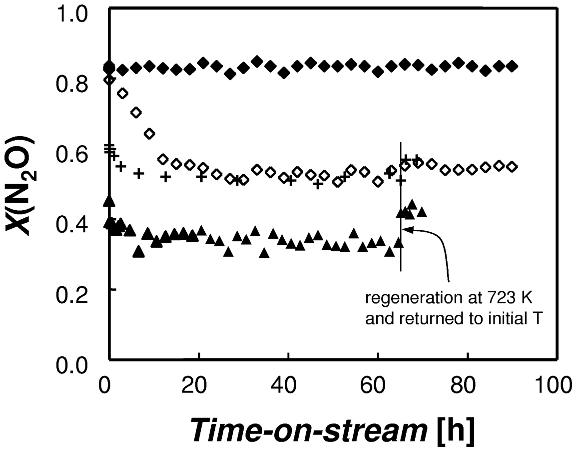

Figure 3. Evolution of N_2O conversion as a function of the time-on-stream for: (▲) ex-Co–La,Al-HTlc (Co/La/Al = 3/1/1, 595 K), (+) ex-Co, Pd–La,Al-HTlc (Co/Pd/La/Al = 3/1/1/1, 580 K), (◇) ex-Co–Rh,Al-HTlc (Co/Rh/Al = 3/0.02/1, 580 K), and (◆) ex-Co,Mg–Rh,Al-HTlc (Co/Mg/Rh/Al = 3/1/0.02/1, 580 K). N_2O feed pressure 1 mbar; space time $W/F^0_{N_2O} = 8.05 \times 10^5$ g s/mol.

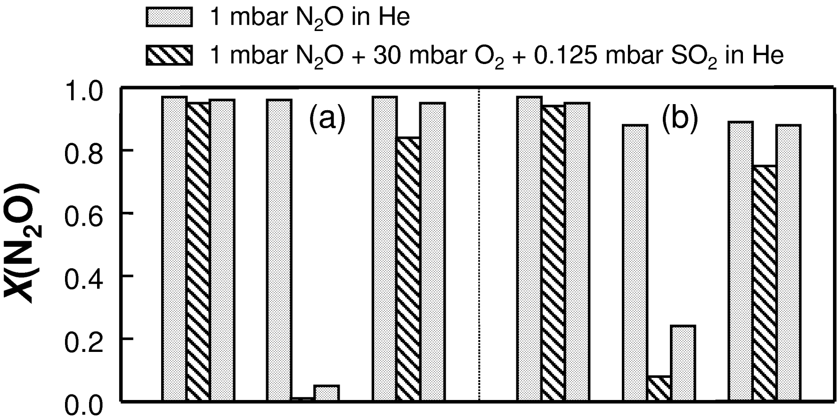

	T [K]	723	595	595	673	595	595
Molar ratios	Co	3	3	3	3	3	3
	Mg	-	-	1	-	-	1
	Pd	-	-	-	1	1	1
	Rh	0.02	0.02	0.02	-	-	-
	La	-	-	-	1	1	1
	Al	1	1	1	1	1	1

Figure 4. Effect of the addition of $SO_2 + O_2$ mixtures on the N_2O conversion for different catalysts and temperatures: (a) Rh- and (b) Pd-containing catalysts. Gas-phase conditions and catalyst formulations are described in the figure. Space time $W/F^0_{N_2O} = 8.05 \times 10^5$ g s/mol.

soning, deactivation) or reversible (a kinetic effect). The high sorbent capacity for SO_x of $MgAl_2O_4$ spinel and the easy reduction/desorption of the sulfates formed [37] may enable the reversible poisoning in our catalysts. Mg can modify the properties of active phase [13], preserving the re-adsorption of the poison on it, once its desorption from the magnesium aluminate spinel takes place.

4. Conclusions

The decomposition of nitrous oxide has been studied over calcined hydrotalcite-like compounds (ex-HTlc's). Addition of different cations to the ex-HTlc's produces a better performance of the catalysts for the decomposition of N_2O, from both activity and stability points of view. In particular, the addition of Pd to the active ex-Co–La,Al-HTlc produces a catalyst with a similar activity than the ex-Co–Rh,Al-HTlc, reported as the most active for the N_2O decomposition in this group. Additionally, ex-Co,Pd–La,Al-HTlc (Co/Pd/La/Al = 3/1/1/1) produces a stable conversion under time-on-stream experiments, while ex-Co–Rh,Al-HTlc (Co/Rh/Al = 3/0.02/1) is partially deactivated. A stabilizing effect arises in SO_2 and O_2 stream when Mg in added to the catalyst structure, leading to reversible inhibition even at low temperature. This is especially attractive for FBC flue-gas conditions.

Acknowledgement

N.M. van der Pers is gratefully acknowledged for his help with the XRD measurements and discussion.

References

[1] P.L. Crutzen, J. Geophys. Res. 76 (1971) 7311.

[2] J.C. Kramlich and W.P. Linak, Prog. Energy Combust. Sci. 20 (1994) 149.

[3] P.L. Crutzen and C.J. Howard, Pure Appl. Geophys. 116 (1978) 497.

[4] F. Kapteijn, J. Rodríguez-Mirasol and J.A. Moulijn, Appl. Catal. B 9 (1996) 25.

[5] Y. Li and J.N. Armor, Appl. Catal. B 1 (1992) L21.

[6] G. Centi, A. Galli, B. Montanari, S. Perathoner and A. Vaccari, Catal. Today 35 (1997) 113.

[7] K. Yuzaki, T. Yarimizu, S. Ito and K. Kunimori, Catal. Lett. 47 (1997) 173.

[8] J. Oi, A. Obuchi, G.R. Bamwenda, A. Ogata, H. Yagita, S. Kushiyama and K. Mizuno, Appl. Catal. B 12 (1997) 277.

[9] K. Yuzaki, T. Yarimizu, K. Aoyagi, S. Ito and K. Kunimori, Catal. Today 45 (1998) 129.

[10] S. Kannan and C.S. Swamy, Appl. Catal. B 3 (1994) 109.

[11] J.N. Armor, T.A. Braymer, T.S. Farris, Y. Li, F.P. Petrocelli, E.L. Weist, S. Kannan and C.S. Swamy, Appl. Catal. B 7 (1996) 397.

[12] J. Oi, A. Obuchi, A. Ogata, G.R. Bamwenda, K. Tanaka, T. Hibino and S. Kushiyama, Appl. Catal. B 13 (1997) 197.

[13] J. Pérez-Ramírez, F. Kapteijn, J. Overeijnder and J.A. Moulijn, Appl. Catal. B (1999), submitted.

[14] C.S. Swamy, S. Kannan, Y. Li, J.N. Armor and T.A. Braymer, US Patent 5,407,652 (1995), to Engelhard Corporation.

[15] W.T. Reichle, US Patent 4,458,026 (1984), to Union Carbide Corporation.

[16] H.P. Klug and L.E. Alexander, *X-Ray Diffraction Procedures* (Wiley, New York, 1970) p. 471.

[17] F. Kapteijn and J.A. Moulijn, in: *Handbook of Heterogeneous Catalysis*, Vol. 3, eds. G. Ertl, H. Knözinger and J. Weitkamp (Wiley, Weinheim, 1996) p. 1359.

[18] F. Kapteijn, G. Marbán, J. Rodríguez-Mirasol and J.A. Moulijn, J. Catal. 167 (1997) 256.

[19] S. Miyata, Clays Clay Miner. 31 (1983) 305.

[20] C.P. Kelkar and A.A. Schutz, Micropor. Mater. 10 (1997) 163.

[21] S. Kannan, S. Velu, V. Ramkumar and C.S. Swamy, J. Mater. Sci. 30 (1995) 1462.

[22] S. Minyata, Clays Clay Miner. 23 (1975) 369.

[23] S. Gusi, F. Pizzoli, F. Trifirò, A. Vaccari and G. Del Piero, in: *Preparation of Catalysts IV*, Stud. Surf. Sci. Catal., Vol. 31, eds. B. Delmon, P. Grange, P.A. Jabobs and G. Poncelet (Elsevier, Amsterdam, 1987) p. 753.

[24] A.L. McKenzie, C.T. Fishel and R.J. Davis, J. Catal. 138 (1992) 547.

[25] J. Pérez-Ramírez, F. Kapteijn and J.A. Moulijn, in preparation.

[26] A. Corma, V. Fornés and F. Rey, J. Catal. 148 (1995) 205.

[27] C. Angeletti, F. Pepe and P. Porta, J. Chem. Soc. Faraday Trans. I 74 (1978) 1595.

[28] A.F. Wells, *Structural Inorganic Chemistry* (Oxford Science Publications, Oxford, 1984) p. 595.

[29] F. Basile, L. Bassini, G. Fornasari, F. Trifirò and A. Vaccari, in: *Preparation of Catalysts VII*, Stud. Surf. Sci. Catal., Vol. 118, eds. B. Delmon, P.A. Jacobs, R. Maggi, J.A. Martens, P. Grange and G. Poncelet (Elsevier, Amsterdam, 1998) p. 31.

[30] K. Kaneda, T. Yamashita, T. Matsushita and K. Ebitani, J. Org. Chem. 63 (1998) 1750.

[31] X. Zhang, A.B. Walters and M.A. Vannice, Appl. Catal. B 4 (1994) 237.

[32] D.A. Hickman and L.D. Lewis, J. Catal. 138 (1992) 267.

[33] M. Machida, A. Sato, H. Inoue, K. Eguchi and H. Arai, Catal. Today 26 (1995) 239.

[34] R.F. Hicks, H. Qi, M.L. Young and R.J. Lee, J. Catal. 122 (1990) 280.

[35] G.K. Boreskov, in: *Catalysis: Science and Technology*, Vol. 3, eds. J.R. Anderson and M. Boudart (Springer, Berlin, 1982) p. 39.

[36] A. Corma, A.E. Palomares and F. Rey, Appl. Catal. B 4 (1994) 29.

[37] M. Waqif, O. Saur, J.C. Lavalley, Y. Wang and B.A. Morrow, Appl. Catal. 71 (1991) 319.